Interaction of Cyclohexanediones with Acetyl Coenzyme-A Carboxylase and an Artificial Target-Site Antibody Mimic: A Comparative Molecular Field Analysis

Steve R. Webb,[†] Gregory L. Durst,[‡] Dan Pernich,[‡] and J. Christopher Hall*[,§]

Dow AgroSciences Canada Inc., 241-111 Research Drive, Saskatoon, Saskatchewan, Canada S7N 3R2; Dow AgroSciences, 9330 Zionsville Road, Indianapolis, Indiana 46268-1054; and Department of Environmental Biology, University of Guelph, Guelph, Ontario, Canada N1G 2W1

Similarities and differences between steric and electrostatic potentials of a monoclonal-antibody-based surrogate of a herbicide target-site and its in vitro enzyme target were investigated using three-dimensional quantitative structure−activity relationship comparative molecular field analysis (3D-QSAR CoMFA). Two separate, five-component, partial least squares CoMFA models were developed to compare the interaction of cyclohexanedione herbicides with their target site, acetyl coenzyme-A carboxylase (ACCase; EC 6.4.1.2) and a cyclohexanedione pharmacophore-specific monoclonal antibody (mAb A). On the basis of CoMFA models, similarities in steric and electrostatic requirements around position 2 of the binding site for the oxime functional group of the cyclohexanedione molecule appear to be crucial for interaction of the herbicide with both ACCase and mAb A. These similarities explain the observed quantitative relationship between binding of cyclohexandedione herbicides to ACCase mAb A. Furthermore, these results support the production and use of mAb-based surrogates of pesticide targets as screening tools in pesticide discovery programs.

Keywords: *Monoclonal; cyclohexanedione herbicides; ACCase; CoMFA*

INTRODUCTION

The discovery of new lead chemistries by pharmaceutical and agrochemical companies is labor-intensive and expensive. Three basic strategies are routinely employed to identify new lead chemistry: random screening, structural modifications of an existing lead, and rational design (Schacter et al., 1992). A common component in all three strategies is the screening of prospective candidate molecules, which can be the rate-limiting step in the discovery of new lead chemistries. Pharmaceutical and agrochemical companies have adopted screening strategies that allow rapid and efficient screening of large numbers of compounds, also known as "high-throughput" screening, to streamline the discovery process (Kleinberg and Wanke, 1995). Assays used for high-throughput screening must be accurate, inexpensive, robust, and amenable to automation. Ideally, the drug or pesticide target is used for the high-throughput screening assay; however, alternative screening methods must be developed when the target site is unknown or unstable or the assay cannot be properly formatted. An alternate approach is to use antibodies as surrogates of the drug or pesticide target site. The rationale for using antibodies as screening tools is based on the observation that antibodies, when produced against small ligands, may demonstrate binding properties similar to those of the natural receptor (Linthicum et al., 1988).

To evaluate the utility of antibodies as screening tools, monoclonal antibodies (mAbs) were produced against a cyclohexanedione−bovine serum albumin immunogen (Webb et al., 1997). Herbicides of the cyclohexanedione structural class are potent inhibitors of plant-derived acetyl coenzyme-A carboxylase (ACCase; EC 6.4.1.2), the first dedicated step in fatty acid biosynthesis (Burton et al., 1991; Rendina and Felts, 1988; Secor and Cseke, 1988). Previously, Webb and Hall (2000a) used a competitive, indirect enzyme-linked immunosorbent assay (ciELISA) with one monoclonal antibody (mAb A) to cluster cyclohexanedione analogues, on the basis of cross-reactivity, into active and nonactive ACCase inhibitors. They also found that mAb A also recognized herbicidally active analogues from the aryloxyphenoxypropanoic acid (Rendina et al., 1995; Secor and Cseke, 1988), indolizine-2,4-dione (Babezinski and Fisher, 1991; Cressman, 1994) and the triazinedione (Walker et al., 1990) structural classes of ACCase inhibitors (Webb and Hall, 2000b). Furthermore, in a pilot screen using a ciELISA and mAb A, Webb and Hall (2000b) identified two novel ACCase inhibitor structures. Although mAb A has qualitative specificity for the ACCase-inhibitor pharmacophore (i.e., herbicide pharmacophore) similar to that of ACCase inhibition, Webb and Hall (2000b) found that there is little quantitative correlation between inhibition of antibody binding and inhibition of ACCase activity.

To better understand the relationship between the interaction of cyclohexanedione herbicides with the mAb-based surrogate of ACCase and the target enzyme, ACCase, three-dimensional quantitative structure−activity relationship comparative molecular field analysis (3D-QSAR CoMFA) models were developed. Our

* Author to whom correspondence should be addressed [telephone (519) 824-4120, ext. 2740; fax (519) 837-0442; e-mail jchall@evbhort.uoguelph.ca].

[†] Dow AgroSciences Canada Inc.

[‡] Dow AgroSciences U.S.A. Inc.

[§] University of Guelph.

10.1021/jf990568v CCC: $19.00
Published on Web 05/12/2000

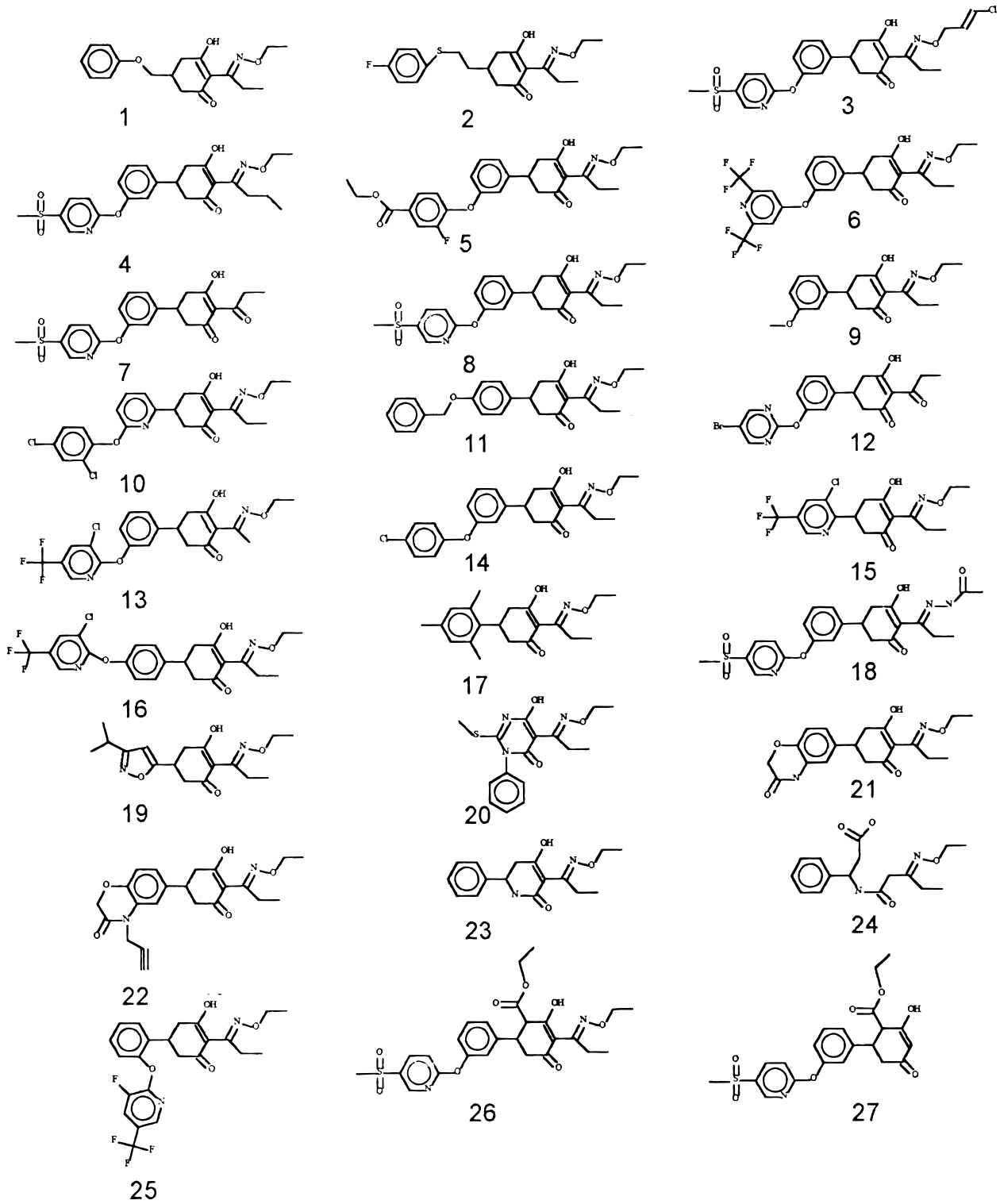

Figure 1. Structures of 27 cyclohexanedione analogues used as a training set to develop the ACCase CoMFA model. The 24 cyclohexanedione analogues used to develop the monoclonal antibody CoMFA training set excluded analogues **12**, **21**, and **22**.

CoMFA models can be used to illustrate the similarities and differences between binding of cyclohexanedione herbicides to ACCase and the mAb-based surrogate of ACCase. The relevance of these similarities and differences to the observed experimental relationship between mAb A and ACCase binding is discussed.

MATERIALS AND METHODS

Molecular Modeling. The structures of the cyclohexanedione analogues and their corresponding inhibitory activity against both ACCase and the monoclonal antibody designated mAb A (Webb et al., 1997; Webb and Hall, 2000b) are shown in Figure 1 and Table 1, respectively. The initial 3D coordinates for the cyclohexanedione structures (Figure 1) were obtained from CONCORD 3.0.1 (University of Texas at Austin) and imported into the molecular modeling program Sybyl 6.1a (Tripos Associates, St. Louis, MO) on an Iris workstation (Silicon Graphics Inc., Mountain View, CA). Partial atomic charges required for the calculation of the electrostatic interactions were calculated using MOPAC 93 (QCPE, Bloomington, IN).

Table 1. Concentration of Cyclohexanedione Analogue Required To Inhibit 50% of Acetyl Coenzyme-A Carboxylase Activity and mAb A Binding (IC_{50})

		IC_{50}, μM	
compd[a]	DEX no.	enzyme[b]	antibody
1	X000304	4.47	nt[c]
2	X001882	1.78	0.144
3	X003789	0.02	0.214
4	X003799	0.71	0.224
5	X007941	0.30	0.069
6	X008096	0.04	0.468
7	X008300	>100[d]	5.248
8	X008416	0.26	0.010
9	X008513	2.57	0.015
10	X009760	0.22	0.016
11	X010131	0.29	0.005
12	X010140	64.56	nt
13	X012232	1.07	0.078
14	X013632	0.10	0.661
15	X015146	3.89	0.004
16	X015450	1.10	0.012
17	X197953	0.33	0.331
18	X199547	>100	58.884
19	X200605	7.76	0.031
20	X209174	>100	38.019
21	X209348	0.71	nt
22	X209826	0.89	nt
23	X210072	36.31	0.035
24	X249639	>100	>100
25	X010765	>100	0.324
26	X006057	11.75	0.933
27	X006515	>100	>100

[a] Cyclohexanedione structures illustrated in Figure 1. [b] Acetyl coenzyme-A carboxylase IC_{50} values provided by C. Cseke (Dow AgroSciences). [c] nt, not tested. [d] IC_{50} value greater than the highest concentration tested (100 μM).

Cyclohexanedione analogue **3** (Figure 1) served as the template molecule for the alignment rule. The atoms forming the cyclohexanedione ring of the other analogues were superimposed on the equivalent atoms in the template molecule using the match function in Sybyl 6.1a. The remaining regions of the molecules were superimposed on the template by altering torsional angles. The aligned molecules were then minimized using the Tripos force field in Sybyl 6.1a. A 3D lattice of 2 Å was constructed around the molecules (Figure 2). An sp^3 carbon probe with a +1 point charge was placed at each lattice point, and the resulting steric (Lennard-Jones) and electrostatic (Coulombic) interactions with each atom in the molecule were calculated and then saved in a CoMFA QSAR table.

The CoMFA QSAR table was constructed with rows containing the molecule names and columns containing the dependent data (log $1/IC_{50}$) as well as the individual steric and electrostatic field potential values at each grid point for each molecule. Partial least squares (PLS) analysis was used to develop the relationship between the independent variables (steric and electrostatic properties) and the IC_{50} values. The predictive ability of each CoMFA model (antibody and ACCase) was determined by the leave-one-out method of cross-validation, in which the activity of each molecule is predicted by a model obtained from the rest of the molecules in the training set. The optimum number of components was determined to be that which yielded the highest cross-validated Q^2 and lowest standard errors. During cross-validation, the QSAR columns (steric and electrostatic values at a given lattice point) were filtered at 0.5 kcal/mol, thereby eliminating what were considered to be noncontributing columns. Non-cross-validated PLS analysis (obtained using all observations in the model) was performed to develop the antibody and ACCase models.

RESULTS AND DISCUSSION

A set of 27 cyclohexanedione analogues (Figure 1), which exhibit some diversity in their structures and activities against both ACCase and mAb A (Table 1), were used for CoMFA analyses. The generic cyclohexanedione-inhibitor structure is illustrated in Figure 3. The core structural features common to all active cyclohexanedione inhibitors are carbonyl, oxyimino, and hydroxyl functional groups at positions 1, 2, and 3 of the cyclohexane ring, respectively (Figure 3; Markley et al., 1995; Webb et al., 1997). The nature and type of substituents at R_1, R_2, R_3, and R_4 are variable when compared to the core structure, and the precise role these substituents play in binding to ACCase is not known (Markley et al., 1995; Webb et al., 1997).

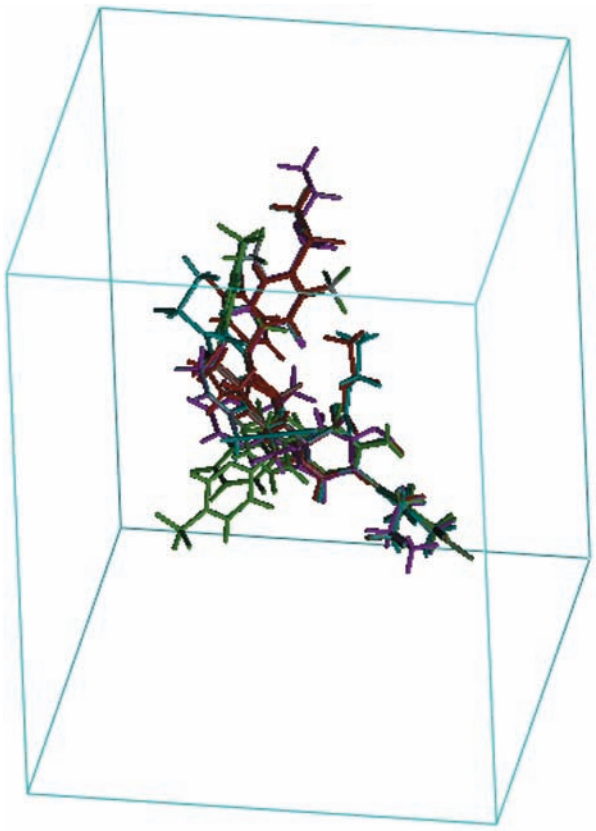

Figure 2. Superimposition of the 27 cyclohexanedione analogues (Figure 1) in the CoMFA lattice.

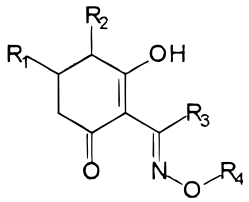

Figure 3. Generic structure of the cyclohexanedione herbicide class.

In the case of ACCase, analysis of a total of 27 cyclohexanedione analogues was used to perform the CoMFA, and the results are summarized in Table 2. The optimum number of components for the ACCase PLS CoMFA model was determined to be five, on the basis of the increase in the cross-validated Q^2 from −0.184 to 0.609 (Q^2; Cramer et al., 1988). The cross-validated Q^2 of 0.609 suggests that this five-component PLS CoMFA model for ACCase would be predictive for cyclohexanedione analogues outside the initial training set. For instance, Cramer et al. (1988) indicate that a PLS CoMFA analysis of any molecular property exhibiting a cross-validated Q^2 value ≥0.3 suggests the prob-

Table 2. Summary of Statistics for CoMFA Models[a]

source	statistic	no. of components[b] 1	2	3	4	5
enzyme	Q^2	−0.184	0.475	0.537	0.575	0.609
	$\pm SE_x$[c]	1.294	0.880	0.844	0.826	0.811
	r^2					0.985
	±SE					0.158
antibody	Q^2	0.004	0.164	0.182	0.144	0.055
	$\pm SE_x$[c]	1.392	1.307	1.326	1.394	1.507
	r^2					0.940
	±SE					0.380

[a] IC_{50} values were generated from effects of 27 and 24 cyclohexanediones on ACCase activity and mAb A binding, respectively. [b] Number of principal components included in the model. [c] Subscript *x* indicates statistics from leave-one-out cross-validation analyses. $n = 27$ for the enzyme model; $n = 24$ for the antibody model.

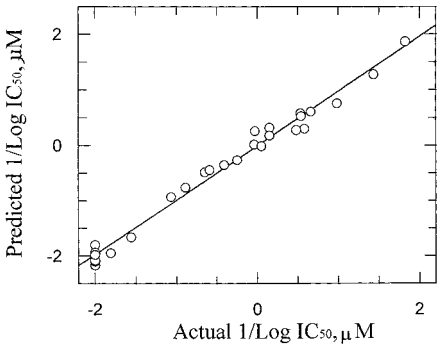

Figure 4. Predicted versus actual log $1/IC_{50}$ values for cyclohexanedione inhibition of ACCase using the five-component PLS model ($r^2 = 0.985$).

ability of correlation by chance between the property and the CoMFA fields examined to be ≤5%. A non-cross-validated CoMFA for ACCase was also conducted to assess how well the CoMFA model fit the experimental data (Table 2). The plot of the actual versus predicted log $1/IC_{50}$ activity of the 27 cyclohexanedione analogues against ACCase is shown in Figure 4. The non-cross-validated r^2 was 0.985 (Table 2) with a slope of 0.97 (Figure 4), indicating the ACCase CoMFA model explains the observed experimental results but does not assess the predictive ability of the model for cyclohexanedione analogues outside the training set.

The mAb CoMFA model was constructed from 24 cyclohexanedione analogues. The cyclohexanedione analogues **12**, **21**, and **22** (Figure 1) were not included in the antibody PLS CoMFA analysis because the cross-reactivity of these analogues with the mAb was assessed differently from the original 24 described by Webb and Hall (2000b). When these three analogues were included in the antibody PLS CoMFA model, there was no apparent relationship between the antibody binding data and the steric and electrostatic potentials (cross-validated $Q^2 = -0.015$). When these analogues were omitted from the analysis, the best cross-validated Q^2 for the antibody PLS CoMFA model was 0.182, with an optimum number of components of three (Table 2). The low cross-validated Q^2 (<0.3) suggests the antibody model would not predict the activity of cyclohexanedione analogues outside the initial 24 analogue training set (Cramer et al., 1988). One possible explanation for the low cross-validated Q^2 of the antibody model may be attributed to the small number of analogues (24 analogues) in the training set, which suggests that the

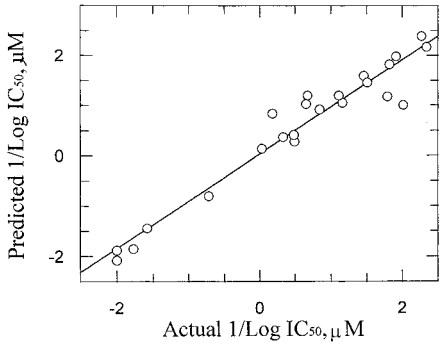

Figure 5. Predicted versus actual log $1/IC_{50}$ values for cyclohexanedione inhibition of antibody binding using the five-component PLS model ($r^2 = 0.940$).

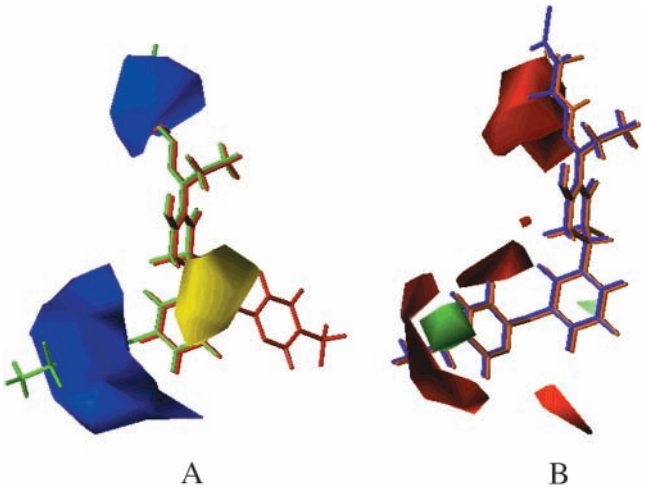

Figure 6. Steric and electrostatic potential of ACCase CoMFA fields. (A) ACCase steric CoMFA field graph showing the active cyclohexanedione analogue **3** (Figure 1) and inactive analogues **25** and **26** (Figure 1). The blue and yellow contours surround regions where steric interactions increase or decrease cyclohexanedione inhibition of ACCase activity, respectively. The contours are shown at 0.023 (blue) and −0.020 (yellow) coefficient levels. (B) ACCase electrostatic potential CoMFA fields showing the active cyclohexanedione analogue **3** and inactive analogue **18** (Figure 1). The red and green contours surround regions where increasing negative charge decreases (red) or increases (green) cyclohexanedione inhibition of ACCase activity, respectively. The contours are shown at 0.025 (red) and −0.024 (green) coefficient levels.

information contributed by each cyclohexanedione analogue is very important to the final antibody model.

A non-cross-validated PLS CoMFA model (Table 2) was developed for the mAb, and the plot of actual versus predicted IC_{50} values for the 24 cyclohexanedione analogues is shown in Figure 5. A non-cross-validated r^2 of 0.940 (Table 2) with a slope of 0.97 (Figure 5) was obtained from the mAb PLS CoMFA model, which indicates the model can account for the observed mAb experimental results.

An important feature of the CoMFA methodology is the ability to visualize the steric and electrostatic fields that correlate with biological activity. The steric and electrostatic field potential graphs generated from the ACCase and mAb CoMFA models are shown in Figures 6 and 7, respectively. In the steric graphs (Figures 6A and 7A), the presence of bulk groups in the blue regions contribute positively to the binding of cyclohexanedione analogues to ACCase and the mAb (favorable interactions), whereas the occupation of space defined by the yellow regions decreases the binding of cyclohexanedi-

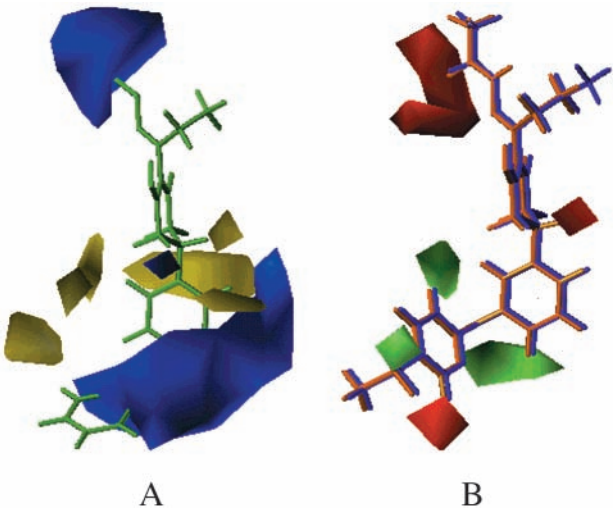

Figure 7. Steric and electrostatic potential antibody CoMFA fields. (A) Antibody steric CoMFA field graph showing the active cyclohexanedione analogue **11** (Figure 1). The blue and yellow contours surround regions where steric interactions increase or decrease cyclohexanedione binding to the mAb, respectively. The contours are shown at 0.018 (blue) and −0.040 (yellow) coefficient levels. (B) Antibody electrostatic potential CoMFA fields showing the active cyclohexanedione analogue **4** and inactive analogue **18** (Figure 1). The red and green contours surround regions where increasing negative charge decreases (red) or increases (green) cyclohexanedione binding to the antibody, respectively. The contours are shown at 0.025 (red) and −0.050 (green) coefficient levels.

one analogues (unfavorable interactions). The steric map for both ACCase and mAb A revealed similar favorable regions (blue) around the oxime functional group and the R_4 substituent at position 2 of the cyclohexanedione ring (Figures 6A and 7A). The ACCase steric map (Figure 6A) suggests that a favorable steric region (blue) is located around the large meta or para substituents on the R_1 aryl ring. This favorable steric region (blue) of ACCase may account for the increased potency of cyclohexanedione analogues that have large aryloxy meta substituents at the position 5 aryl ring (e.g., analogues **3**, **5**, and **6**; Figure 1; Table 1) when compared to analogues with small methyl or methoxy substituents (analogues **9** and **17**; Figure 1; Table 1). The mAb model also contained a favorable steric region (blue) around the larger meta or para substituents of the position 5 aryl ring (Figure 7A), but this favorable steric region (blue) was much smaller and not as continuous when compared to the ACCase steric graph (Figure 6A). These differences between the ACCase and antibody steric graphs may account for the lack of quantitative correlation between IC_{50} values for inhibition of both mAb A binding and ACCase activity by each cyclohexanedione analogues.

The ACCase steric map (Figure 6A) revealed the presence of an unfavorable steric region (yellow) near the R_2 ethyl ester substituents of analogues **26** and **27** (Figure 1). The location of this unfavorable steric region (yellow) also explains the inactivity of analogue **25** (Figure 1; Table 1). The large 3-fluoro-5-(trifluoromethyl)-2-pyridinyloxy substituent at the ortho position of the R_1 aryl ring of analogue **25** penetrates this unfavorable steric region (yellow) and may account for the inactive nature of this analogue against ACCase. In contrast, the steric graph of the antibody model (Figure 7A) contained three small unfavorable steric regions (yellow), none of which corresponded to the size or location of the yellow region on the ACCase steric map (Figure 6A). These differences in the location and size of the unfavorable steric regions (yellow) when the ACCase and antibody steric graphs are compared (Figures 6A and 7A) may explain the differences in the response of mAb A and ACCase to analogue **25** (Table 1; Webb and Hall, 2000b).

The electrostatic potential graphs for the ACCase and mAb CoMFA models are shown in Figures 6B and 7B, respectively. A negative potential in the green regions and a positive potential in the red regions indicate increased cyclohexanedione binding to both ACCase and mAb A (Figures 6B and 7B). For instance, red areas define regions where decreasing negative charge enhances cyclohexanedione binding and, conversely, green areas define regions where increasing negative charges increases the binding of cyclohexanediones to both the antibody and ACCase. The majority of the ACCase and antibody electrostatic potential maps are defined by red areas where decreasing the negative charge results in increased cyclohexanedione binding (Figures 6B and 7B). The green areas on the ACCase and antibody electrostatic potential graphs are small and discontinuous, which suggests that increasing the negative charge of cyclohexanedione analogues does not increase binding to either the enzyme or antibody (Figures 6B and 7B). The red regions around the position 2 oxime functional group and R_4 substituent for both the enzyme and antibody electrostatic potential graphs (Figures 6B and 7B) are similar. This red area defines a region on the ACCase and antibody models that requires decreasing negative charge for cyclohexanedione binding. The location of this region may account for the inactivity of analogue **18** (Figure 1) against both ACCase and mAb A (Table 1). Analogue **18** is not active because the oxime functional group has been replaced with an acylhydrazone substituent (Figure 1). Both electrostatic potential graphs suggest the presence of the acylhydrazone substituent would result in an unfavorable electrostatic interaction with both ACCase and the antibody (Figures 6B and 7B).

Our CoMFA models illustrate the similarities and differences in steric and electrostatic potential between interaction of cyclohexanediones with ACCase and mAb A. The enzyme and antibody CoMFA models have similar steric and electrostatic potentials located around the position 2 oxime functional group and R_4 substituents (Figures 6 and 7). These similarities may account for the qualitative relationship between cyclohexanedione inhibition of mAb A and ACCase. These similarities may also account for the ability of mAb A to cross-react with the other structural classes of ACCase inhibitors (Webb and Hall, 2000b). For example, Rendina et al. (1995) suggested that the aryloxyphenoxypropanoic acid structural classes of ACCase inhibitors overlap through the oxime region of the cyclohexanediones. It is likely that the similarities in the antibody and enzyme steric and electrostatic potentials at the oxime region may account for antibody recognition of aryloxyphenoxypropanoic acid structural class of inhibitors. Furthermore, mAb A recognition of the indolizidine-2,4-dione and triazinedione structural classes of inhibitors suggests that these two structural classes may also overlap with the cyclohexanediones in a similar manner. Additional studies are required to test and confirm these hypoth-

eses about the overlap of the different structural classes of ACCase inhibitors within the ACCase pharmacophore.

ABBREVIATIONS USED

ACCase, acetyl coenzyme-A carboxylase; CoMFA, comparative molecular field analysis; PLS, partial least squares; 3D-QSAR, three-dimensional quantitative structure function activity relationship; mAb, monoclonal antibody.

ACKNOWLEDGMENT

S.R.W. was the recipient of an NSERC graduate student fellowship.

LITERATURE CITED

Babezinski, P.; Fischer, R. Inhibition of acetyl-coenzyme A carboxylase by the novel grass-selective herbicide 3-(2,4-dichlorophenyl)-perhydroindolizine-2,4-dione. *Pestic. Sci.* **1991**, *33*, 455−466.

Burton, J. D.; Gronwald, J. W.; Keith, R. A.; Somers, D. A.; Gengenbach, B. G.; Wyse, D. L. Kinetics of inhibition of acetyl-coenzyme A carboxylase by sethoxydim and haloxyfop. *Pestic. Biochem. Physiol.* **1991**, *39*, 100−109.

Cramer, III, R. D.; Patterson, D. E.; Bunce, J. D. Comparative molecular field analysis (CoMFA). I. Effect of shape on binding of steroids to carrier proteins. *J. Am. Chem. Soc.* **1988**, *110*, 5959−5967.

Cressman, E. N. K. Synthesis of an indolizidinedione oxime inhibitor of acetyl coenzyme-A carboxylase (ACCase). *Bioorg. Med. Chem. Lett.* **1994**, *4*, 1983−1984.

Kleinberg, M. L.; Wanke, L. A. New approaches and technologies in drug design and discovery. *Am. J. Health-Syst. Pharm.* **1995**, *52*, 1323−1336.

Linthicum, D. S.; Bolger, M. B.; Kussie, P. H.; Albright, G. M.; Linton, T. A.; Combs, S.; Marchetti, D. Analysis of idiotypic and anti-idiotypic antibodies as models of receptor and ligand. *Clin. Chem.* **1988**, *34*, 1676−1680.

Markley, L. D.; Geselius, T. C.; Hamilton, C. T.; Secor, J.; Swisher, B. A. Aryloxy- and pyridyloxyphenylcyclohexanedione grass herbicides: Synthesis and herbicidal activity. In *Synthesis and Chemistry of Agrochemicals IV*; Baker, D. R., Fenyes, J. G., Basarab, G. S., Eds.; ACS Symposium Series 584; American Chemical Society: Washington, DC, 1995; pp 220−233.

Rendina, A. R.; Felts, J. M. Cyclohexanedione herbicides are selective and potent inhibitors of acetyl-CoA carboxylase from grasses. *Plant Physiol.* **1988**, *86*, 983−986.

Rendina, A. R.; Campopiano, O.; Marsilii, E.; Hixon, M.; Chi, H.; Taylor, W. S.; Hagenah, J. A. Overlap between herbicidal inhibitors of acetyl coenzyme-A carboxylase: Enhanced binding of cyclic triketones, a novel class of graminicide. *Pestic. Sci.* **1995**, *43*, 368−371.

Schacter, L. P.; Anderson, C.; Caretta, R. M. Drug discovery and development in the pharmaceutical industry. *Semin. Oncol.* **1992**, *19*, 613−621.

Secor, J.; Cseke, C. T. Inhibition of acetyl-CoA carboxylase activity by haloxyfop and tralkoxydim. *Plant Physiol.* **1988**, *86*, 10−12.

Walker, K. A.; Ridley, S. M.; Lewis, T.; Harwood, J. L. A new class of herbicide which inhibits acetyl-CoA carboxylase in sensitive plant species. *Biochemistry* **1990**, *29*, 3743−3747.

Webb, S. R.; Hall, J. C. A monoclonal-based ELISA for the identification of herbicidal cyclohexanedione analogues that inhibit graminaceous acetyl-coenzyme A carboxylase. *J. Agric. Food Chem.* **2000a**, *48*, 1210−1218.

Webb, S. R.; Hall, J. C. Development and evaluation of an immunological approach for the identification of novel acetyl coenzyme-A carboxylase inhibitors: assay optimization and pilot screen results. *J. Agric. Food Chem.* **2000b**, *48*, 1219−1228.

Webb, S. R.; Lee, H.; Hall, J. C. Cloning and expression in *Escherichia coli* of an anti-cyclohexanedione single chain variable (ScFv) antibody fragment and comparison to the parent monoclonal antibody. *J. Agric. Food Chem.* **1997**, *45*, 535−541.

Received for review May 28, 1999. Revised manuscript received March 28, 2000. Accepted March 28, 2000. Financial support from the Natural Sciences and Engineering Research Council (NSERC) of Canada and Agriculture and Agri-food Canada (AAFC) to J.C.H. is gratefully acknowledged. We thank Dow AgroSciences for technical and financial support.

JF990568V